

# Aging mechanisms and lifetime of PEFC and DMFC

Shanna D. Knights\*, Kevin M. Colbow, Jean St-Pierre, David P. Wilkinson

*Ballard Power Systems, 9000 Glenlyon Parkway, Burnaby, BC, Canada V5J 5J9*

## Abstract

This paper provides an overview of several operating conditions which can have a significant effect on the durability of polymer electrolyte fuel cells (PEFCs) and direct methanol fuel cells (DMFC), including: low reactant flows, high and low humidification levels, and high and low temperatures. The possible effects of these conditions, along with possible mitigating strategies, are discussed. Data from various tests are presented demonstrating lifetimes from 1000 h to greater than 13,000 h for various conditions and applications.

© 2003 Elsevier B.V. All rights reserved.

*Keywords:* Polymer electrolyte fuel cells; Direct methanol fuel cells; Lifetime; Aging mechanisms; Failure; Mitigation strategies

## 1. Introduction

Fuel cell systems, when properly designed, can be a reliable and durable method to produce efficient and environmentally friendly energy for various applications. As polymer electrolyte fuel cells (PEFCs) approach commercialization, significant progress is being made towards producing systems that achieve the optimum balance of cost, efficiency, reliability and durability.

Fuel cell lifetime requirements vary significantly, ranging from 3000 to 5000 operating hours for car applications, up to 20,000 operating hours for bus applications and up to 40,000 operating hours for stationary applications. There can be various lifetime requirements for other types of applications, such as portable power, un-interrupted power supply (UPS), etc. Degradation rate requirements are normally set based on beginning-of-life (BOL) performance, end-of-life (EOL) performance requirements, and lifetime durability requirements in terms of operational hours and/or stand-by hours. The degradation range of 2–10  $\mu\text{V}/\text{h}$  is common for most applications.

The most common fuel for the PEFC is hydrogen, which can be either in an essentially pure gas stream or in the form of reformat produced from various fuels, such as methane, methanol, and gasoline. A special case of PEFCs is that of direct methanol fuel cells (DMFC), which convert methanol directly into electrical energy, without the use of a reformer. Wasmus [1] provides an overview of DMFC technology. Such systems offer many advantages in terms of

system simplicity and will likely be preferred for a number of niche markets, but development lags hydrogen based PEFCs. Degradation rates of DMFCs are generally higher than that of hydrogen PEFCs, and depend on the application, but are typically in the range of 10–25  $\mu\text{V}/\text{h}$ .

The ability of the fuel cell to operate under a wide range of operating conditions with different system characteristics is described by the term, “fuel cell operational flexibility”. Optimum fuel cell operational flexibility must take into account both specified and an estimated amount of unexpected, or “out-of-specification” conditions over the fuel cell target lifetime. Some of the conditions to consider include: reactant flow rates and composition, operating and environmental temperature, operating and environmental pressure, humidification levels, peak load requirements and turn-down ratios, duty-cycle characteristics (including percentage of time at different load points), and required rate of transient responses.

Due to the absence of moving parts, the fuel cell is an inherently reliable system, but can be prone to material degradation from the presence of: reactants; various materials, including catalyst; significant electrical potential and current density; and various operating conditions, including temperature and pressure ranges. The management of the fuel cell stack for lifetime is dependent on how these components and interacting conditions are designed and managed. As a very general statement, the lifetime achieved in a fuel cell can often be traded-off against another characteristic, such as operating regime, cost, and power density. Targeted lifetime and failure testing can be conducted during the development stage, to provide the basis to understand potential failure mechanisms and develop the necessary technology to mitigate such mechanisms. Therefore, a fuel cell system

\* Corresponding author. Tel.: +1-604-412-3152; fax: +1-604-453-3782.  
E-mail address: [shanna.knights@ballard.com](mailto:shanna.knights@ballard.com) (S.D. Knights).

may be custom designed to meet the needs of a particular application, including a target lifetime requirement.

This paper will provide an overview of some operational conditions that can affect fuel cell lifetime. The conditions to be discussed include: low reactant flows, high and low humidification levels, and high and low temperatures. Each of these conditions and associated failures can be discussed in much more depth, but is beyond the scope of this paper. For a discussion on the effects of water management, please refer to the paper by St-Pierre et al. [2]. For a literature review of PEFC durability, please refer to the discussion by Wilkinson and St-Pierre [3].

## 2. Experimental

Various standard Ballard fuel cells and fuel cell stacks were used to generate the data presented in this paper, with active areas ranging from 49 to 1280 cm<sup>2</sup>. Tests were conducted on single-cells or short-stacks (typically in the range of 4–20 cells). The conditions used varied with the application and are noted with the data when relevant. Standard Ballard test equipment, including humidifier, test station, gas mixer, and electronic load, was used for control of operating conditions.

Fuel starvation was induced by replacing the fuel with humidified nitrogen. An external power supply was used to simulate the stack power to drive the current through the cell or short-stack. External humidifiers were used for humidification experiments, with control of humidification level through adjustment of dew point temperature. Lifetime tests were generally conducted by applying a constant load (unless otherwise stated) over a fixed period of time. During the lifetime, voltage performance points were recorded continuously. Diagnostic tests were generally conducted throughout the test period, but are not shown on the charts. Only operational hours are included in the lifetime calculations. Freeze–thaw data was collected by running a cell through a repetitive cycle, consisting of operation at two different load points, removal of the load and gases, cool down and purging of the cell, freezing, then warm-up and re-introduction of gases and load.

## 3. Discussion

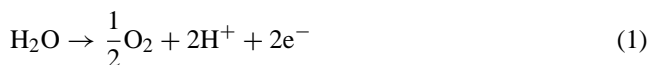
### 3.1. Low reactant flow

High reactant utilization is generally required for most applications in order to maximize fuel efficiency and reduce system parasitic load, size, and weight that may be associated with the oxidant and fuel delivery and/or storage systems. Transient operation, particularly under the demanding conditions of automotive applications, introduces greater challenges due to rapid load changes and the resulting wide range of conditions.

During high overall stack utilization, uneven flow sharing between cells can result in partial fuel and/or air starvation conditions in individual cells. This situation can be exacerbated by the presence of liquid water in channels or other blockages, resulting in further flow sharing difficulties that in extreme cases can lead to complete starvation conditions. One example of such a condition is sub-zero start-up or operation. As long as the stack temperature remains below zero, the cells are prone to ice formation and subsequent flow channel blockage. Although the stack and system operation can be designed to reduce these occurrences, it is generally accepted that rapid heating of the stack to minimize ice formation is desirable.

In the case of oxidant starvation, the protons passing through the membrane will combine, in the absence of oxygen, to form hydrogen, and the cell essentially acts as a hydrogen pump. The cathode potential drops due to the lack of oxygen and the presence of hydrogen, and the cell voltage generally drops to very low levels or may even become negative.

In the case of fuel starvation, if hydrogen is no longer available to be oxidized, the anode potential will rise to that required to oxidize water, assuming water is available, resulting in the evolution of oxygen and protons at the anode, according to:



The protons will pass through the membrane and combine with oxygen at the cathode in the normal reduction reaction to produce water (reverse of reaction (1)).

A polarization of a complete fuel starvation (no hydrogen) with humidified nitrogen flowing on the anode is presented in Fig. 1 for an anode with a 4 mg Pt/cm<sup>2</sup> loading of Pt black catalyst on the anode. The cell voltage, as measured from the cathode to the anode, drops due to a rise in anode potential, which reaches levels sufficient for water oxidation, i.e. >1.23 V. The values of the cathode and anode potential are

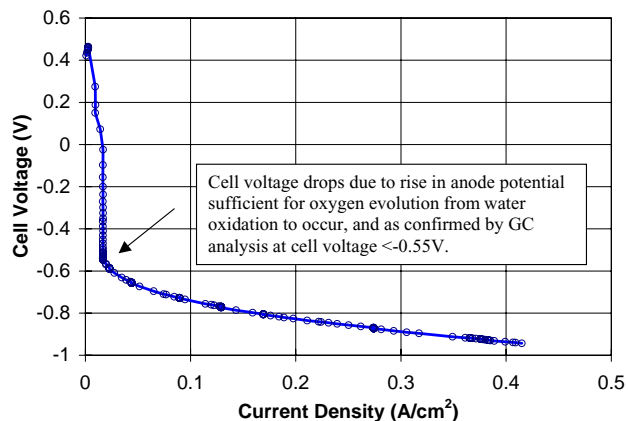


Fig. 1. Fuel starvation polarization. Humidified anode/cathode feed streams: nitrogen/air. 3 bar, 75 °C, 4 mg/cm<sup>2</sup> Pt on each of cathode and anode.

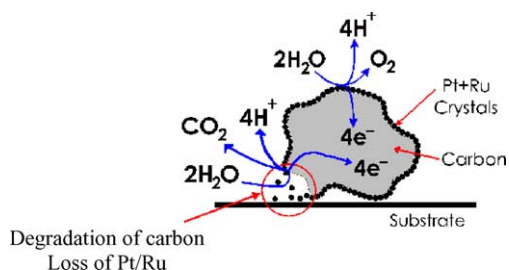
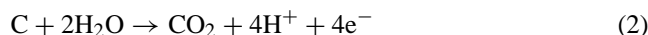


Fig. 2. Schematic representation of degradation of carbon catalyst support during operation in the absence of fuel.

not individually known, but the presence of oxygen on the anode due to reaction (1) was confirmed by gas chromatographic (GC) analysis, indicating that high anode potentials are being achieved.

Most current technology development is focussed on the use of platinum (or platinum and ruthenium) supported on carbon particles, in order to reduce the amount of platinum required on the anode down to 0.05–0.45 mg/cm<sup>2</sup>, and as described in [4]. These types of anodes are prone to degradation during fuel starvation due to reaction (2), the oxidation of carbon, which is catalyzed by the presence of platinum [5]. This reaction proceeds at an appreciable rate at the electrode potentials required to electrolyze water in the presence of platinum (greater than approximately 1.4 V [6]).



This is shown schematically in Fig. 2. The catalyst support is converted to CO<sub>2</sub>, and Pt and/or Ru particles may be lost from the electrode, resulting in loss of performance.

Reduced degradation can be achieved through modification of the anode structure to favour oxidation of water over carbon. Some strategies to accomplish this include: enhanced water retention on the anode (e.g. through modifications to PTFE and/or ionomer, and addition of water blocking components such as graphite); use of improved catalysts to reduce the required anode potential for water electrolysis and thus the associated carbon oxidation (e.g. additional Ru on the anode); use of a more robust catalyst support (e.g. more graphitic carbon or alternative support materials); and increased catalyst coverage on the support to reduce contact of carbon with reactants (e.g. higher weight percentage Pt on the carbon) [7–10].

Fig. 3 shows the cell voltage response over time of four different four-cell stacks with different anode designs. Each stack was subjected to fuel starvation conditions through an equivalent number of cycles. Each stack was then finally starved of hydrogen and allowed to go into voltage reversal until an average cell voltage of –2 V was reached. The length of time the cells operated prior to reaching –2 V is a measure of robustness to fuel starvation.

### 3.2. Low humidification

Water management is key to optimum reliability and durability of fuel cells. Inadequate water content, either globally

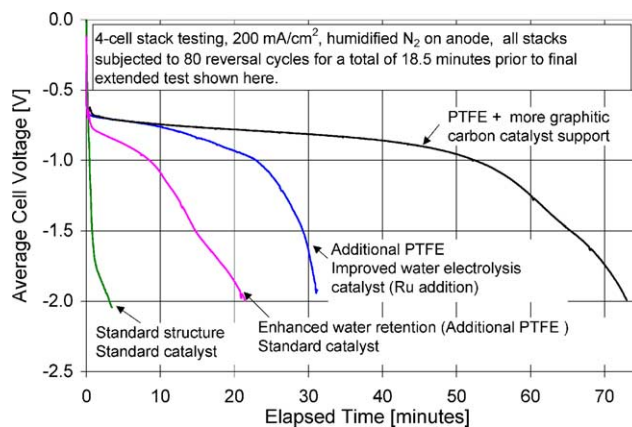


Fig. 3. Comparison of different anode structures in severe failure testing. Each cell has equivalent cathode (~0.7 mg/cm<sup>2</sup> Pt, supported on carbon). Testing conducted at 200 mA/cm<sup>2</sup>, fully humidified nitrogen on anode. Anode loading at ~0.3 mg/cm<sup>2</sup> Pt supported on carbon (varied materials and compositions). Each curve represents the results from a four-cell stack with each cell in the stack of identical composition. Four separate stack tests were run to generate the curves.

within the stack or locally at certain locations within the unit cell, results in reduced conductivity in the membrane and in any ionomer present in the catalyst layer. This results in increased ohmic losses and a drop in cell voltage. This effect can be demonstrated by conducting controlled tests on a cell design that has not been optimized for low humidification conditions. The results of such a test are shown in Fig. 4. The cell is initially running fully humidified with a constant performance. Once a step-change is made through a reduction in humidification level, the performance quickly drops. The drier the conditions, the greater the loss in performance. When the humidification level is subsequently increased, the performance quickly recovers.

Inadequate water content can also accelerate membrane physical degradation, and can ultimately result in membrane holes and reactant gas crossover. This effect was observed through a series of tests in which the same type of

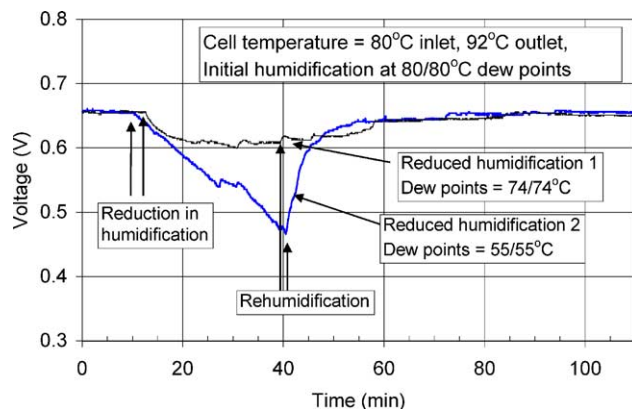


Fig. 4. Effect of reduced humidification levels on non-optimized cell design. Air/hydrogen operation with specified humidification levels. Current density: 1 A/cm<sup>2</sup>.

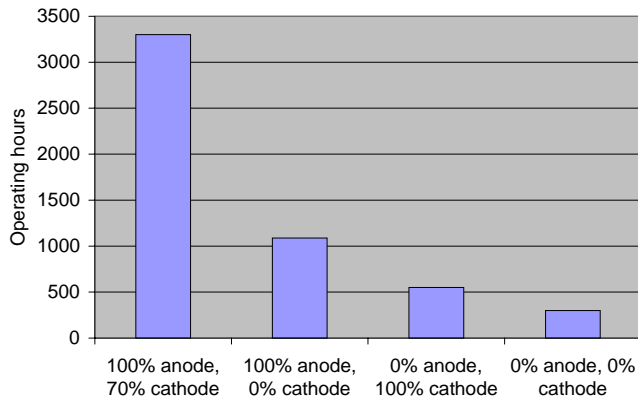


Fig. 5. Time to significant gas crossover ( $>10\text{ cm}^3/\text{min}$  at 2 bar pressure differential) as a function of inlet gas humidification for a non-optimized cell design. Air/hydrogen operation, current density:  $540\text{ mA}/\text{cm}^2$ , coolant temperature:  $75^\circ\text{C}$ , humidification levels of reactant streams as indicated.

non-optimized cell design was run under varying humidification conditions. The results of these tests are shown in Fig. 5, where, as conditions become drier, failure due to significant reactant gas crossover occurs after shorter lifetimes.

It is possible to continue running a cell with membrane holes present, but the performance becomes very sensitive to pressure differentials across the membrane. In this case, the reactants are able to transfer across the membrane, and dilute or consume the opposite reactant. When this occurs, either fuel or air starvation can result, depending on the direction of the pressure differential. Fig. 6 shows a lifetime plot for an eight-cell stack during which a large crossover leak developed in one cell. The stack was operated with the fuel pressure slightly higher than the air pressure, resulting in air starvation in that cell. It can be observed that the cell voltage dropped to negative values, but continued operation for approximately 500 h prior to the end of the lifetime test. The remaining cells in the stack continued to operate with stable voltages for the entire planned 3000 h test duration.

Improved water management can be achieved through various strategies. One challenge faced by cell and stack

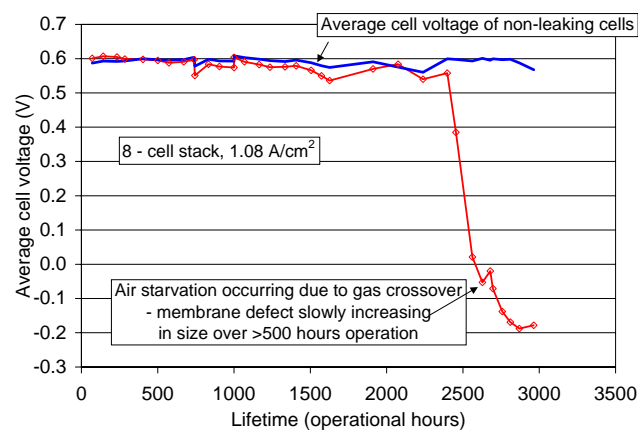


Fig. 6. Lifetime test showing effect of membrane damage resulting in gas crossover. Air/hydrogen operation.

designers is how to effectively distribute the product water within the cell. Unless the inlet gas streams are fully humidified, the inlet region will have low humidity. High oxygen concentration at the inlet can also result in high catalytic activity in this region, which, when combined with the reduced water for heat transfer removal, can result in increased local temperatures. The combined effects of low humidification and locally increased temperatures can result in a region prone to membrane failure. Conversely, as the product water accumulates, the back portion of the cell may be fully saturated, leading to the possibility of two-phase flow and potential mass transport losses, contamination, and flow sharing issues.

One of the easiest strategies to implement to redistribute product water within the cell is through operation with counter-current reactant flows, essentially using the MEA as an in-cell humidifier [2,11,12]. A study was conducted to determine the optimum flow configuration for drier conditions (no air humidification, fuel humidification at  $10^\circ\text{C}$  lower than the inlet coolant temperature). The strategies tested included co- and counter-flow strategies for the three fluid streams: air, fuel, and coolant. In this case, the cell was operated with a  $15^\circ\text{C}$  temperature differential from inlet to outlet in the coolant stream. Operation with fuel counter-flow to air and coolant achieved the most stable performance and the lowest cell resistance. Fig. 7 shows a lifetime test run under these conditions, with no degradation observed. The other configurations tested resulted in a steady decrease in cell voltage and the accompanying increase in cell resistance, indicating the effect was due to membrane drying, resulting in proton conductivity loss.

### 3.3. High humidification

While insufficient humidification can introduce problems for durability and reliability, excess humidification can also cause many potential problems. Excess humidification may result from several scenarios. During transient operation,

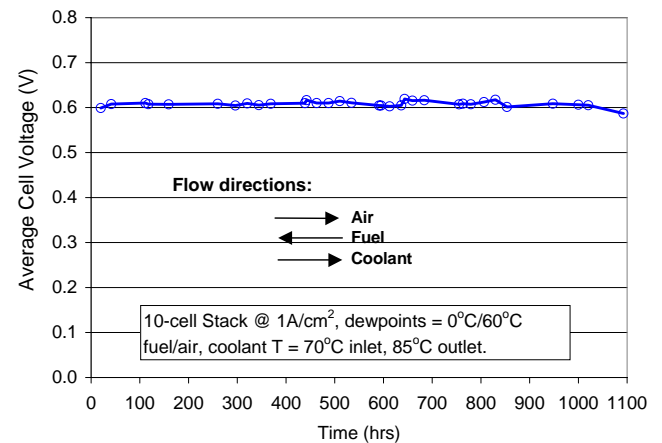


Fig. 7. Stable lifetime performance achieved using counter-flow operation. Ten-cell stack, hydrogen/air operation.

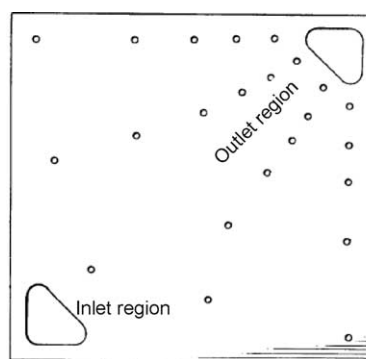


rapid electrical load changes may be demanded of the fuel cell. The change in operating conditions may lag behind that of the load and the conditions can become temporarily non-optimized. This situation may cause flooding or drying conditions to exist in the stack. Stack and system design must be carefully optimized to ensure uniform temperatures throughout the stack. Any local regions of lower temperature have the potential to cause associated water condensation and/or pooling. The use of reformed fuel is generally associated with a large fuel water content which in some cases may result in greater than 100% saturation upon being cooled to stack temperature if the moisture is not adequately removed prior to entering the stack. A more fundamental problem with the fuel cell is the production of water as the gases are consumed, resulting in the tendency for product water to accumulate in the back half of the cell. In most applications, the fuels are run with low gas flows to minimize parasitic losses, which may be inadequate to completely vaporize and/or entrain all of the water produced, although various strategies exist to reduce oversaturation [12,13].

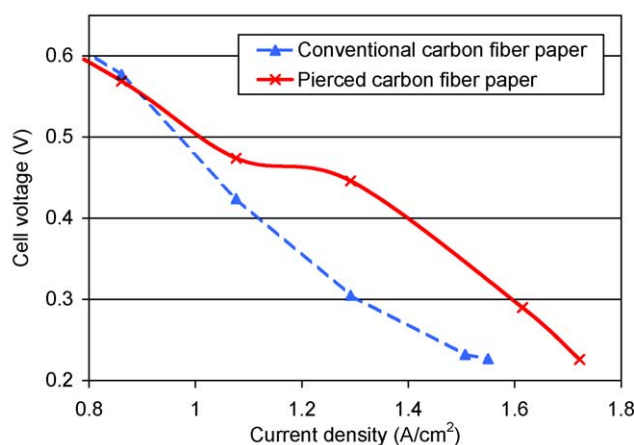
Excess water content, if not properly managed, can result in reactant diffusion blockages, particularly on the cathode, causing an increase in mass transport losses. Excess water can also increase flow-sharing issues, which becomes particularly significant when running under low flows. A further effect of excess water is the increase in contaminants that may be leached out of system/stack components, and the increased opportunities to transfer these to the cell. This has resulting degradation effects, such as a reduction in hydrophobicity in the cell, which further exacerbates the effects of increased water content [2]. Other contamination effects may include loss of membrane conductivity, loss of active catalyst sites, and increased mass transport losses.

Many of the strategies for mitigation of excess water are similar to those used to reduce the impact of drying conditions. The product and humidification water must be properly distributed throughout the cell and between cells. Strategies which can be used include reactant flow strategies (such as counter-flow design discussed previously), flowfield and plate design, and MEA design [14].

One example of MEA design to mitigate the product water accumulation is the use of a non-uniform in-plane electrode structure to improve water retention in the drier inlet regions, and enhance water removal in the wetter outlet regions [2,14,15]. This strategy minimizes both dry and flooded regions. This may be achieved through a localized increase in electrode gas diffusion layer (GDL) substrate porosity in areas where water accumulates, such as the oxidant outlet. Fig. 8 shows one example of electrode design and performance improvements achieved at high current densities [14,15]. In this case, the GDL contains added perforations, with increased density of perforations in the wetter outlet region. The performance is equivalent in the low current density region, but shows a significant improvement to conventional GDL design in the region of greater than 1 A/cm<sup>2</sup>, which is typically limited by mass transport losses.



(a)



(b)

Fig. 8. Water management through MEA design. (a) Plan view of MEA showing perforations in GDL with increased perforation density in wetter outlet region. (b) Performance of MEA at increased current density compared to a conventional, non-pierced MEA design.

A particular case where water management is of high importance is that of direct methanol fuel cells (DMFC). Although the cathode reactions in a DMFC are the same as that of hydrogen based fuel cells, the fuel consists of a methanol and water mixture, usually introduced into the anode in the liquid phase. DMFCs do not suffer from issues with dry regions due to the liquid fuel, but are particularly prone to cathode flooding. A significant portion of the liquid water in the fuel stream will ultimately cross over to the cathode. This results in increased cathode mass transport losses due to the difficulty of the reactants to diffuse through water vapour and/or liquid present which must be removed by the cathode gas stream.

As a result of liquid fuel feed, DMFCs require different water management strategies than hydrogen based PEMFCs. One strategy that can be used to recover performance loss is load cycling. When operating under constant load, the cells tend to suffer high performance degradation due to an increase in gas diffusion limitations as water builds up on the cathode. This can be seen in the polarization curves of Fig. 9. A cell operating for only 16 h under constant current load has lost significant performance at high current densities, indicative of mass transport losses due to gas diffusion

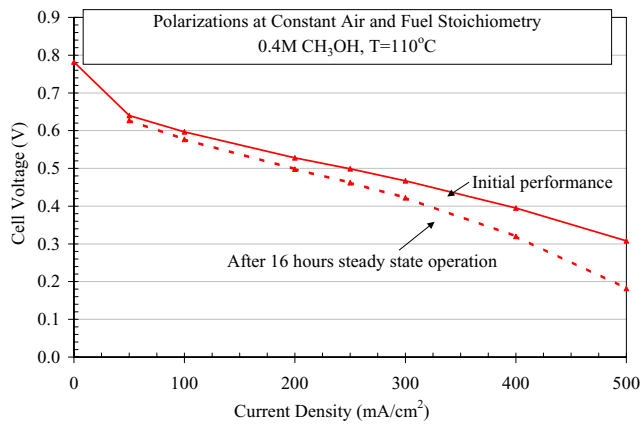


Fig. 9. Performance of a DMFC after 16 h of steady state operation compared to initial performance.

limitations. Quantification of this increased loss can be accomplished through testing of the cell in the high current density region on each of two different oxidants, air and a mixture, termed “helox”, consisting of 21% oxygen and 79% helium. The voltage response as a function of current density and oxidant used provides information on gas diffusion limited performance, with an increasing gap at high current densities indicating increased losses [2,16]. The change in gas diffusion limited performance of a DMFC run continuously for only 16 h is compared in Fig. 10 against one run under load cycling for almost 2000 h. These cells suffered a change in gas diffusion limited performance of  $\sim 370$  and  $\sim 35\%$ , respectively, an order of magnitude improvement in degradation. The load cycling strategy used in this case consists of removing the load from the cell for 30 s during every 30 min operational period. As can be observed given the results in Fig. 10, this has proven to be very effective in main-

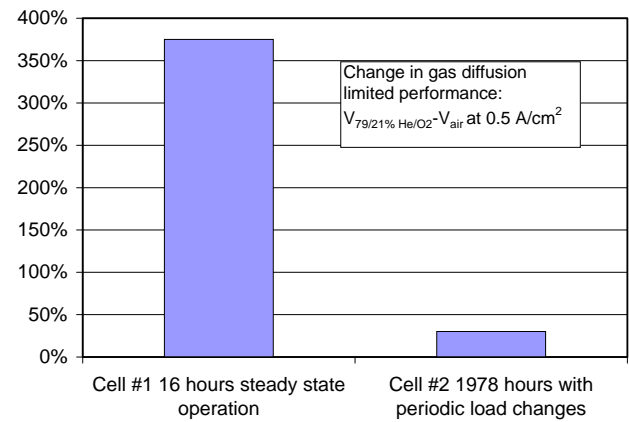


Fig. 10. Comparison of change in gas diffusion limited performance in a DMFC depending on operational strategy used. Gas diffusion limited performance is defined as the difference in cell voltage on air as compared to a mixture of 79%  $O_2$ /21%  $N_2$  at  $0.5 A/cm^2$ .

taining low degradation rates. In Fig. 11, a DMFC lifetime plot at  $0.2 A/cm^2$ , during which the load cycling strategy was used, is presented. The lifetime performance was very good for this type of fuel cell, with a degradation rate of only  $13 \mu V/h$  for almost 2000 h with no failures. It is important to note that many DMFC applications can also achieve these low degradation rates simply due to the dynamic nature of load conditions, including on–off cycles.

### 3.4. Low temperature

A wide range of operating temperatures is required for fuel cells, depending on the application. For automotive applications, this may include sub-zero operation upon start-up in freezing temperatures [17]. Regardless of the start-up requirements, the stack and system will likely be required

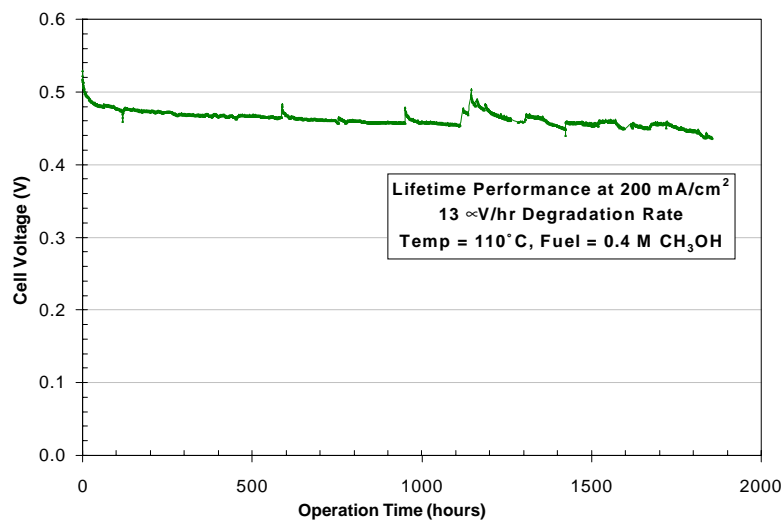


Fig. 11. Lifetime performance of a direct methanol fuel cell using load cycling strategy to reduce mass transport related degradation. 30 s of open circuit voltage operation/30 min of on-load operation.

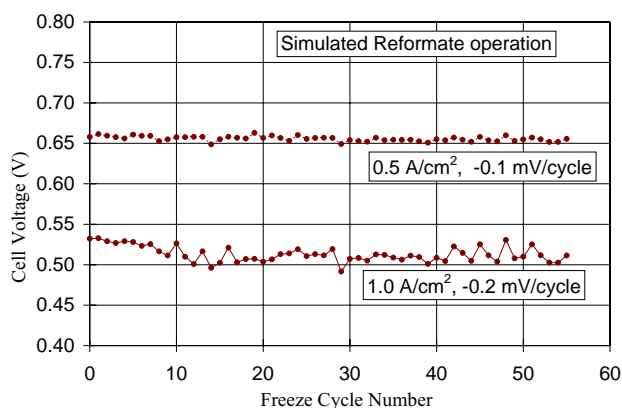


Fig. 12. Effect of freeze–thaw cycles on fuel cell performance. Simulated reformate operation. Operation and purging conducted between each purge/thaw cycle.

to withstand many freeze–thaw cycles. Possible low temperature effects can include: reduced material degradation rates; increased contamination effects, e.g. carbon monoxide, which is generally present in reformed fuel, is adsorbed much more strongly at lower temperatures [18]; lower performance due to increased kinetic, ohmic, and reactant transport losses; and increased importance of water management. Water management is particularly important for sub-zero operation, as water blocking channels may freeze, resulting in partial or complete reactant starvation in some cells.

One mitigation strategy that can be used for operation when sub-zero temperatures are expected, is purging of flow channels. This is an effective technique to clear the channels of water prior to freezing [19]. Fig. 12 shows the performance of a cell after each of 55 freeze–thaw cycles, with operation and purging during each cycle. No significant performance loss is observed at  $0.5 \text{ A/cm}^2$ , and at  $1.0 \text{ A/cm}^2$  a loss of only  $0.2 \text{ mV/cycle}$  is observed. This is consistent with data reported in [20], in which no degradation was observed when the cell was cooled to  $-78^\circ\text{C}$ , and with that reported in [21], in which three freeze–thaw cycles to  $-10^\circ\text{C}$  were completed with no observable degradation.

### 3.5. High temperature

Operation of the fuel cell at increased temperature has several advantages. Higher temperatures result in reduced cooling requirements, which is particularly important for automotive applications in which engine size can be limited by radiator capacity [22]. Higher temperatures are preferred for co-generation of heat and electricity, which is particularly advantageous for residential applications. Contaminants tend to adhere less strongly to the catalyst and other fuel cell components as the temperature is increased. For example, carbon monoxide present in reformed fuel has less poisoning effect at higher temperatures. However, the disadvantages can include: increased material degradation rates and associated contaminant levels; and, a reduction in mem-

brane and ionomer moisture content for a given set of operational conditions [23]. The last effect can result in loss of performance due to decreased proton conductivity and increased membrane degradation leading to holes and/or thin spots.

The use of reformed fuel provides an example of a localized high temperature effect that has the potential to reduce lifetime of the fuel cell. The use of a small stream of air bleed into the fuel is often used to recover the CO induced anode catalyst poisoning by oxidizing the CO to  $\text{CO}_2$  [24]. However, the presence of this air bleed can result in localized hot spots generally close to the fuel flow channel inlet area, depending on the cell design. Failure analysis of the problem region is important to detect any link between the failure and specific features of the flow channel design [25]. The use of modeling techniques can be further used to determine the most likely contributing factors, such as coolant channel location, plate conductivity, air and coolant channel locations, interactions with MEA design, etc. In this way, the cell can be designed to prevent the occurrence of hot spots and extend the lifetime of the fuel cell under these conditions.

An example of the improvement achievable using this approach is represented in Fig. 13. In this case, the application was the Ballard 250 kW Natural Gas Power plant. In an early design, the cells began to fail very early for this type of application; at 5000 h for MEA type 1 and in less than 2000 h for MEA type 2. In this case, the MEA type 2 was the preferred design in all other respects. Thus, the strategy mentioned above of failure analysis and modeling was accomplished to highlight key contributors to the early failures. Subsequent redesign and testing resulted in very significant improvements to durability, particularly with the target MEA type 2. In laboratory simulation trials, a short stack (17-cells) operated for over 13,000 h without failure, with an average cell degradation rate of only  $0.5 \mu\text{V/h}$ , as presented in Fig. 14. In a field trial under dynamic operation, the full power plant operated for 7400 h, to the end of the field trials, with no MEA failures.

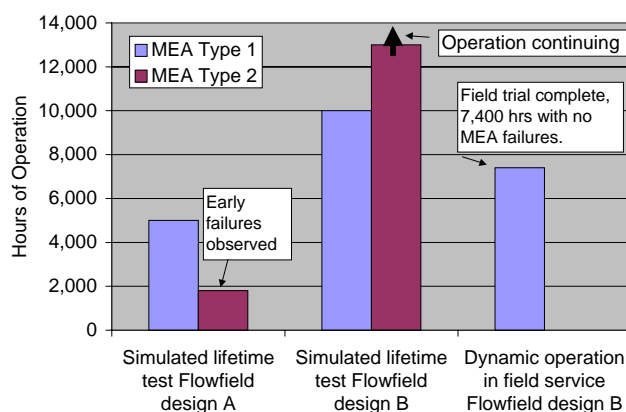


Fig. 13. Comparison of lifetimes achieved in 250 kW natural gas power plant hardware. Air/simulated reformate operation with 2% air bleed.

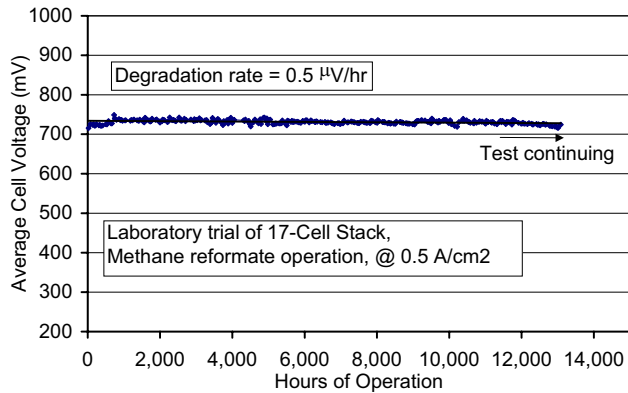


Fig. 14. Lifetime test of 17-cell stack comprised of 250kW natural gas power plant hardware. Coolant operating temperature: 82°C at stack outlet. Design of cell optimized to minimize localized high temperature effects at membrane in fuel inlet. Actual temperature at membrane is not measured.

#### 4. Conclusions

An overview of the effect of various operational conditions on the durability of the fuel cell was presented. Lifetime can be extended both through control of these conditions, within application and system abilities, and through optimized design to reduce the impact of these conditions. Fundamental understanding of failure mechanisms and development of mitigating technology is facilitated by directed lifetime and failure testing throughout the technology development cycle. Various lifetime plots were presented showing very stable performance. Although DMFC is at an earlier stage of development, significant progress has been made in achieving good durability, and it is a prime candidate for niche markets with moderate lifetime requirements.

#### Acknowledgements

The authors would like to acknowledge the following groups within Ballard Power Systems for generating and providing much of the data shown and discussed: R&D Department, Product Development Reliability Group, and Field Testing Personnel.

#### References

- [1] S.K.A. Wasmus, J. Electroanal. Chem. 461 (1999) 14–31.
- [2] J. St-Pierre, D.P. Wilkinson, S. Knights, M.L. Bos, J. N. Mater. Electrochem. Sys. 3 (2000) 99–106.
- [3] D.P. Wilkinson, J. St-Pierre, Durability, in: W. Vielstich, H. Gasteiger, A. Lamm (Eds.), Handbook of Fuel Cells: Fundamentals, Technology and Applications, vol. 3, Wiley, 2003, pp. 611–626 (Chapter 47).
- [4] P. Costamagna, S. Srinivasan, J. Power Sources 102 (2001) 242–252.
- [5] E. Passalacqua, M. Vivaldi, N. Giordano, P.L. Anotonucci, K. Kinoshita, in: Proceedings of the 27th Intersociety Energy Conversion Engineering Conference, vol. 929294, 1992, pp. 3.425–3.431.
- [6] R.E. Billings, The Hydrogen World View, American Academy of Science, 1991.
- [7] S.D. Knights, D.P. Wilkinson, S.A. Campbell, J.L. Taylor, J.M. Gascoyne, T.R. Ralph, PCT WO 01/15247 A2, 1 March 2001.
- [8] J.L. Taylor, D.P. Wilkinson, D.S. Wainwright, T.R. Ralph, S.D. Knights, PCT WO 01/15249 A2, 1 March 2001.
- [9] S.D. Knights, J.L. Taylor, D.P. Wilkinson, S.A. Campbell, PCT WO 01/15254 A2, 1 March 2001.
- [10] S.D. Knights, J.L. Taylor, D.P. Wilkinson, D.S. Wainwright, PCT WO 01/15255 A2, 1 March 2001.
- [11] D.P. Wilkinson, H.H. Voss, N.J. Fletcher, M.C. Johnson, E.G. Pow, United States Patent 5,773,160 (June 30 1998).
- [12] J. St-Pierre, D.P. Wilkinson, H. Voss, R. Pow, in: O. Savadogo, P.R. Roberge (Eds.), New Materials for Fuel Cell and Modern Battery Systems II, Ecole Polytechnique, Montreal, 1997, pp. 318–329.
- [13] N.J. Fletcher, C.Y. Chow, E.G. Pow, B.M. Wozniczka, H.H. Voss, G. Hornburg, D.P. Wilkinson, United States Patent 5,547,776 (20 August 1996).
- [14] D.P. Wilkinson, J. St-Pierre, J. Power Sources 113 (2003) 101–108.
- [15] M.C. Johnson, D.P. Wilkinson, C.P. Asman, M.L. Bos, R.J. Potter, United States Patent 5,840,438 (24 November 1998).
- [16] Y.W. Rho, S. Srinivasan, Y.T. Kho, J. Electrochem. Soc. 141 (1994) 2084–2096.
- [17] R. Sims, I.F. Jr. Kuhn, Cold Weather Operational Considerations for Direct Hydrogen, Automotive Fuel Cell Systems.
- [18] Jr. T.A. Zawodzinski, C. Karupiah, F. Uribe, S. Gottesfeld, in: J. Mc Breen, S. Mukherjee, S. Srinivasan (Eds.), Proceedings of the 1st International Symposium of the Electrochemical Society, Electrode Materials and Processes for Energy Conversion and Storage IV, PV 97-13, Montreal, Canada, May 1997, The Electrochemical Society, Pennington, NJ, pp. 139–149.
- [19] J. Roberts, J. St-Pierre, M. van Der Geest, A. Atbi, N. Fletcher, WO 01/24296, 5 April 2001.
- [20] S.F. Simpson, C.E. Salinas, A.J. Cisar, O.J. Murphy, Factors affecting the performance of proton exchange membrane fuel cells, in: A. Landgrebe, S. Gottesfeld, G. Halpert (Eds.), Proceedings of the 1st International Symposium of the Electrochemical Society, First International Symposium on Proton Conducting Membrane Fuel Cells, PV 95-23, Hardbound, Chicago, Illinois, The Electrochemical Society, Pennington, NJ, pp. 182–192 (English).
- [21] M.S. Wilson, J.A. Valerio, S. Gottesfeld, Electrochim. Acta 40 (1995) 355–363.
- [22] M. Sadler, A.J. Stapleton, R.P.G. Heath, N.S. Jackson, Fuel Cell Power for Transportation, SP-1589, SAE, vol. 81–90, March 2001.
- [23] A. Sen, K.E. Leach, R.D. Varjian, Determination of water content and resistivity of perfluorosulfonic acid fuel cell membranes, in: D.H. Doughty, B. Vyas, T. Takamura, J.R. Huff (Eds.), Proceedings of the Materials Research Society Symposium on the Materials for Electrochemical Energy Storage and Conversion: Batteries Capacitors and Fuel Cells, vol. 393, 17 April 1995, pp. 157–162 (English).
- [24] S. Gottesfeld, J. Pafford, J. Electrochem. Soc. 135 (1988) 2651–2652.
- [25] G. Lamont, D. Wilkinson, United States Patent 5,763,765 (9 June 1998).